The role of autophagy in high-fat diet-induced insulin resistance of adipose tissues

Yovita Permata Budi [Equal first author, 1, 2] , Yi-Hsuan Li [Equal first author, 3] , Chien Huang [3] , Mu-En Wang [4] , Yi-Chun Lin [5] , De-Shien Jong [3] , Chih-Hsien Chiu [Corresp., 3] , Yi-Fan Jiang [Corresp. 1, 2]

1 Graduate Institute of Molecular and Comparative Pathobiology, National Taiwan University, Taipei, Taiwan

2 School of Veterinary Medicine, National Taiwan University, Taipei, Taiwan

3 Department of Animal Science and Technology, National Taiwan University, Taipei, Taiwan

4 Department of Pathology, Duke University, North Carolina, Durham, United States

5 Department of Animal Science, National Chung Hsing University, Taichung, Taichung, Taiwan

Corresponding Authors: Chih-Hsien Chiu, Yi-Fan Jiang
Email address: chiuchihhsien@ntu.edu.tw, yfjiang@ntu.edu.tw

Aims: Studies have observed changes in autophagic flux in the adipose tissue of type 2 diabetes patients with obesity. However, the role of autophagy in obesity-induced insulin resistance is unclear. We propose to confirm the effect of High-Fat Diet (HFD) on autophagy and insulin signaling transduction from adipose tissue to clarify whether altered autophagy-mediated HFD induces insulin resistance, and to elucidate the possible mechanisms in autophagy-regulated adipose insulin sensitivity.

Methods: 8-week-old male C57BL/6 mice were fed with HFD to confirm the effect of HFD on autophagy and insulin signaling transduction from adipose tissue. Differentiated 3T3-L1 adipocytes were treated with 1.2 mM Fatty Acids (FAs) and 50 nM Bafilomycin A1 to determine the autophagic flux. 2.5 mg/kg body weight dose of Chloroquine (CQ) in PBS was locally injected into mouse epididymal adipose (10 and 24 hours) and 40 µM of CQ to 3T3-L1 adipocytes for 24 hours to evaluate the role of autophagy in insulin signaling transduction.

Results: The HFD treatment resulted in a significant increase in SQSTM1/p62, Rubicon expression, and C/EBP Homologous Protein (CHOP) expression, yet the insulin capability to induce Akt (Ser473) and GSK3β (Ser9) phosphorylation were reduced. PHLPP1 and PTEN remain unchanged after CQ injection. In differentiated 3T3-L1 adipocytes treated with CQ, although the amount of phospho-Akt stimulated by insulin in the CQ-treated group was significantly lower, CHOP expressions and cleaved caspase-3 were increased and Bafilomycin A1 induced less accumulation of LC3-II protein.

Conclusion: Long-term high-fat diet promotes insulin resistance, late-stage autophagy inhibition, ER stress, and apoptosis in adipose tissue. Autophagy suppression may not affect insulin signaling transduction via phosphatase expression but indirectly causes insulin resistance through ER stress or apoptosis.

1   **Research Article**

2   **Title: The Role of Autophagy in High-Fat Diet-Induced**
3   **Insulin Resistance of Adipose Tissues**

5   **Authors names and affiliations:**

6   Yovita Permata Budi[1,2*], Yi-Hsuan Li[3*], Chien Huang[3], Mu-En Wang[4], Yi-Chun Lin[5], De-Shien

7   Jong[3], Chih-Hsien Chiu[3†], Yi-Fan Jiang[1,2†]

8   [1] Graduate Institute of Molecular and Comparative Pathobiology, School of Veterinary

9   Medicine, National Taiwan University, Taipei, Taiwan.

10 [2] School of Veterinary Medicine, National Taiwan University, Taipei 10617, Taiwan

11 [3] Department of Animal Science and Technology, National Taiwan University, Taipei, Taiwan.

12 [4] Department of Pathology, Duke University School of Medicine, Duke University, Durham,

13 North Carolina, United States.

14 [5] Department of Animal Science, National Chung Hsing University, Taichung, Taiwan.

15 [*]The authors contributed equally to this study

16 [†]Corresponding Author: Chih-Hsien Chiu and Yi-Fan Jiang

17 Mailing address: Rm. 104-1, No.1, Sec. 4, Roosevelt Road, Taipei City 10617, Taiwan

18 Email: chiuchihhsien@ntu.edu.tw / yfjiang@ntu.edu.tw

Abstract

Aims: Studies have observed changes in autophagic flux in the adipose tissue of type 2 diabetes patients with obesity. However, the role of autophagy in obesity-induced insulin resistance is unclear. We propose to confirm the effect of High-Fat Diet (HFD) on autophagy and insulin signaling transduction from adipose tissue to clarify whether altered autophagy-mediated HFD induces insulin resistance, and to elucidate the possible mechanisms in autophagy-regulated adipose insulin sensitivity.

Methods: 8-week-old male C57BL/6 mice were fed with HFD to confirm the effect of HFD on autophagy and insulin signaling transduction from adipose tissue. Differentiated 3T3-L1 adipocytes were treated with 1.2 mM Fatty Acids (FAs) and 50 nM Bafilomycin A1 to determine the autophagic flux. 2.5 mg/kg body weight dose of Chloroquine (CQ) in PBS was locally injected into mouse epididymal adipose (10 and 24 hours) and 40 μM of CQ to 3T3-L1 adipocytes for 24 hours to evaluate the role of autophagy in insulin signaling transduction.

Results: The HFD treatment resulted in a significant increase in SQSTM1/p62, Rubicon expression, and C/EBP Homologous Protein (CHOP) expression, yet the insulin capability to induce Akt (Ser473) and GSK3β (Ser9) phosphorylation were reduced. PHLPP1 and PTEN remain unchanged after CQ injection. In differentiated 3T3-L1 adipocytes treated with CQ, although the amount of phospho-Akt stimulated by insulin in the CQ-treated group was significantly lower, CHOP expressions and cleaved caspase-3 were increased and Bafilomycin A1 induced less accumulation of LC3-II protein.

Conclusion: Long-term high-fat diet promotes insulin resistance, late-stage autophagy inhibition, ER stress, and apoptosis in adipose tissue. Autophagy suppression may not affect insulin signaling transduction via phosphatase expression but indirectly causes insulin resistance through ER stress or apoptosis.

Introduction

44   Although studies show that interaction of genetic and lifestyle factors cause type 2

45   diabetes (T2D), approximately 90% of people with T2D are overweight or obese (Coops &

46   White, 2012). Adipocyte hypertrophy in obesity will induce the impairment of insulin sensitivity

47   and the overexpression of some inflammatory cytokines that make the adipocyte dysfunctional.

48   The pathway begins with the activation of the insulin receptor tyrosine kinase (IR) by insulin,

49   which phosphorylates and recruits different substrate adaptors such as the Insulin Receptor

50   Substrate (IRS) family of proteins. Tyrosine phosphorylated IRS then displays binding sites for

51   numerous signaling partners. Among them, PI3K has a significant role in insulin function,

52   mainly via the activation of the Akt/PKB and the PKC cascades. Activated Akt induces glycogen

53   synthesis by inhibiting GSK-3, protein synthesis via mTOR and downstream elements, and cell

54   survival by inhibiting several pro-apoptotic agents. Akt phosphorylates and directly inhibits

55   FoxO transcription factors. Inactivation of the receptor responses has been reported as the

56   underlying cause of impaired insulin action (Coops & White, 2012). PHLPP directly

57   dephosphorylates AKT at its hydrophobic motif (Ser473). Additionally, mutations in PTEN have

58   been reported to cause insulin resistance and obesity (Pal et al., 2012). NHERF1 binds directly to

59   PTEN and PHLPP1/2 via the PDZ domain and scaffolds ternary complexes at the membrane to

60   suppress the activation of the PI3K–AKT pathway (Molina et al., 2012).

61   Recent studies have indicated extracellular disturbances, such as excess nutrient

62   inflammation or hyperinsulinemia, cause intracellular stress in adipose tissues, which may

63   damage these cells' ability to perform standard metabolic actions on insulin (Fazakerley et al.,

64   2019). Concerning these intracellular stresses, some studies have identified autophagy as playing

65   a vital role in regulation. Yin et al. (2015) showed that autophagy inhibition caused severe ER

66   stress in adipocytes and thus induced adaptive responses to extracellular disturbances,

67   attenuating insulin resistance deterioration (Zhou et al., 2009). Due to its ability to suppress

68   insulin receptor signaling, ER stress has been proposed as an important factor in peripheral

69   insulin resistance and type 2 diabetes (Ozcan U et al., 2004).

70   During autophagosome biogenesis in macroautophagy, two ubiquitin-like systems, LC3

71   processing and Atg5-Atg12 conjugation, are associated with expanding the phagophore

72   membrane (Yang & Klionsky, 2009). As for LC3, it is located on the membrane after post-

73   translational modifications. The C-terminal end of the cytosolic form LC3-I is cleaved by Atg4,

74   which is then activated by Atg7 and transferred to Atg3. Finally, a phosphatidylethanolamine

75   (PE) will be conjugated to LC3-I to form LC3-II by Atg3 (Kabeya et al., 2004; Hanada et al.,

76   2007). As for the Atg5-Atg12-Atg16 complex system, it promotes the formation of LC3-II

77   (Romanov et al., 2012), which, in addition to participating in autophagosome formation, also has

78   the function of recognizing autophagic cargos. LC3-II acts as a receptor to interact with the

79   adaptor on the targets to promote their uptake and degradation. One of the best-characterized

80   adaptor molecules is p62/SQSTM1, a multifunctional adaptor that enables the turnover of

81   ubiquitinated substrates (Glick, Barth & Macleod, 2010). After expanding the phagophore

82   membrane and cargo engulfment, the mature autophagosome fuses with lysosome to form

83   autolysosome for cargo degradation (Mizushima, 2007).

84   However, all of the above processes presuppose that the autophagy is still normal in the

85   cells, but in the study of Soussi et al. (2015), the autophagy in adipocytes from obese patients

86   may be damaged. The connection between impaired autophagy and insulin resistance was

87   observed by Guo et al. (2017), who showed that Atg7 knockdown in 3T3-L1 adipocytes caused a

88   reduction in the phosphorylation capacity of both the insulin receptor β subunit and IRS-1

89   stimulated by insulin. As insulin resistance progresses, adipocyte autophagy is impaired in

90   insulin-resistant states, in which type 2 diabetics demonstrate increased levels of autophagy-

91   related proteins including ATG5, ATG7, BECN1, LC3-II, and LC3-I as well as autophagosome

92   accumulation was observed in subcutaneous and visceral adipose tissue of non-diabetic obese

93   and T2D patients as compared to lean individuals (Rodríguez A et al., 2012; Kosacka et al.,

94   2015). Moreover, Cai et al. (2018) also found that Akt was not activated by insulin in the white

95   adipose tissue in an AdiAtg3KO mouse model, indicating that early-stage inhibition autophagy

96   accelerated the decline in insulin sensitivity. However, the physiological function of damaged

97   autophagy in adipose is unclear, including its role played in insulin resistance development.

98   Therefore, this study was designed to confirm the effect of HFD on autophagy and insulin

99   signaling transduction from adipose tissue. We then clarified whether altered autophagy-

100 mediated HFD induces insulin resistance. Afterward, we elucidated the possible mechanisms in

101 autophagy-regulated adipose insulin sensitivity.

102 **Materials & Methods**

103 **Animal**

104 In this study, 8-week-old male C57BL/6 mice (obtained from the Laboratory Animal Center,

105 College of Medicine, National Taiwan University) were housed at $25 \pm 2°C$, with an approximate

106 50-60% relative humidity and 12-hour light/12-hour dark cycle. Diets and water are freely

107 accessed. Mice were acclimated for one month before the treatments started and placed in the

108 cage according to their experimental group. Each cage contained 4-6 mice and was provided

109 with enrichment (i.e. plastic tube, shredded paper, etc.). The cage will be cleaned and checked

110 every week. After the treatment, the mice were anesthetized with 2.5% avertin (0.15 mL/10 g)

111 through intraperitoneal injection and sacrificed by cervical dislocation. All the operations on and

112 the usage of animals followed the National Institutes of Health Guide for the Care and Use of

113 Laboratory Animals (NIH Publications No.8023, advised 1978), and were approved by the

114 National Taiwan University Institutional Animal Care and Use Committee (NTU105-EL-00178).

115 High-fat diet-induced T2D in mice

116 B6 mice were randomly grouped to control diet (CTD) or high-fat diet (HFD) groups for 8 (n=4)

117 and 16 weeks (n=6). The CTD and HFD were commercially available diets purchased from

118 Research Diets (Product Number: D12450J and D12492). Before sacrifice at the 16th week, the

119 mice were injected with insulin intraperitoneally for 30 minutes, and blood samples were

120 collected from the orbital sinus. After blood sample collection, mice were sacrificed by cervical

121 dislocation for tissue harvest.

122 Local chloroquine injection in epididymal adipose

123 The 12-week-old male C57BL/6 mice (n=4) were anesthetized with 2.5% avertin (0.15 mL/10 g)

124 through intraperitoneal injection, followed by surgery. The identified epididymal adipose tissues

125 were injected with a 2.5 mg/kg body weight dose of chloroquine (Sigma-Aldrich) in PBS or PBS

126 alone as the control (n=6). As a result of its suitability for in vivo study, chloroquine is used most

127 frequently in mice to assess autophagic inhibition, as well as its affordability compared to

128 Bafilomycin A1 (Moulis et al., 2017). Mice were injected with insulin and sacrificed for tissue

129 harvest at 10 and 24 hours after surgery.

130 Cell culture

131 3T3-L1 preadipocytes were purchased from Taiwan Bioresource Collection and Research Center

132 (BCRC number: 60159). Cells were cultured in high glucose Dulbecco's modified eagle medium

133 (DMEM) (D5648, Sigma-Aldrich; 12100046, Gibco) containing 10% newborn calf serum

134 (16010159, New Zealand origin, Gibco), 1% penicillin-streptomycin (15140122, Gibco) and 2.5

135 g/L of $NaHCO_3$. Cells were maintained at 37℃ with 5% CO2 supplement. For cell maturation,

136   3T3-L1 preadipocytes were switched to a medium that contained 10% fetal bovine serum

137   (10270106, South American origin, Gibco) when the cells were 70% confluent. The medium was

138   also added with 1 μM dexamethasone, 0.5 mM methyl isobutyl xanthine (IBMX), and 1 μg/mL

139   insulin. After 2 days of treatment, the cells were maintained in insulin-only treatment until they

140   were fully differentiated. 50 nM Bafilomycin (Tocris) and a dose of 2.5 mg/kg body weight of

141   chloroquine were added to the culture medium for 4 and 24 hours in 3T3-L1 mature adipocytes

142   and treated insulin 15 minutes before sampling. A hydrophobic fluorescent dye Nile red was

143   used to observe the oil droplet accumulation in 3T3-L1 mature adipocytes after the treatment.

144   Additionally, we treated differentiated 3T3-L1 adipocytes with Bafilomycin A1 and FA. A

145   mixture of 0.6 mM palmitic acid (PA) and 0.6 mM oleic acid (OA) was used to treat 3T3-L1

146   cells for 48 hours. A mixture of OA and PA was dissolved in ethanol, and 1% BSA was added to

147   the culture medium.

148   **Protein sample preparation and Western blotting analysis**

149   Adipose tissues were homogenized in Pierce IP Lysis Buffer (87787, ThermoFisher Scientific)

150   containing complete EDTA-free Protease Inhibitor Cocktail (04693132001, Roche) and

151   PhosSTOP (04906845001, Roche), and then centrifuged at 4℃, 16000×g for 20 minutes. Using

152   Pierce BCA Protein Assay Kit (23225, ThermoFisher Scientific), the samples were diluted and

153   mixed with 4X Laemmli Sample Buffer (1610747, Bio-Rad) and 10 mM dithiothreitol (DTT) to

154   give a final concentration of 2 μg/μL. As for the cell experiment, 3T3-L1 cells were rinsed once

155   with PBS and collected directly in 1X Laemmli Sample Buffer plus 10 mM DTT after treatment.

156   All harvested samples were immediately boiled at 98℃ for 10 minutes and then stored at -20℃.

157   Sodium dodecyl sulfate-polyacrylamide gel electrophoresis (SDS-PAGE) was conducted to

158   separate proteins with different molecular weights, depending on the target protein's size.

159 Precision Plus Protein Dual Color Standards (1610374, Bio-Rad) and protein samples were

160 loaded into gel wells. Electrophoresis was performed using running buffer (25 mM Tris, 192 mM

161 glycine, 0.1% SDS), and the voltages were set at 95 V and 110 V according to the sample during

162 the stacking and resolving stages.

163 After electrophoresis, the separated proteins were transferred onto methanol-pre-wetted and

164 transfer buffer-pre-equilibrated PVDF membrane (1620177, Bio-Rad) via the transfer buffer (25

165 mM Tris, 192 mM glycine, 20% methanol). The protein size was determined by either Trans-

166 Blot Turbo Semi-dry Transfer System (170-4155, Bio-Rad) or Criterion Wet Transfer Blotter

167 (170-4070, Bio-Rad). The proteins were transferred at 25 V constant voltage with 0.4 A for 35

168 minutes for semi-dry transfer. For wet transfer, gels were equilibrated in transfer buffer for 15

169 minutes to remove excessive SDS, and then the proteins were transferred at 70 V with 250 mA

170 for 1 hour.

171 PVDF membranes were washed with methanol and stained with Ponceau S solution to visualize

172 the transferred proteins. The fragment membranes cut at the target position were blocked with

173 5% non-fat milk in TBST and incubated with target protein-specific primary antibodies (Table

174 1), which were diluted with 1% BSA in TBST overnight at 4℃. Membranes were washed with

175 TBST three times for 15, 10, and 10 minutes each and then incubated with the species-specific

176 HRP-conjugated secondary antibodies (1:2500 to 1:5000 diluted with 5% non-fat milk in TBST)

177 for 1 hour at room temperature. Membranes were washed with TBST three times for 10, 5, and 5

178 minutes each, and then the blotting images were visualized with Bio-Rad (1705061) and GE

179 (RPN2235) ECL substrates reagents using a Bio-Rad ChemiDoc Touch Imaging System.

180 Blotting quantification was performed using Bio-Rad Image Lab software. Table 1 presents

181 details about the antibodies.

182 **RNA extraction**

183 The RNA from mouse adipose tissues was extracted using TRIzol reagent (15596018,

184 ThermoFisher Scientific), which was homogenized at 4℃. Afterward, the lysates were added to

185 100 μL of chloroform and then shook for 15 seconds. After being incubated for 2-3 minutes at

186 room temperature, mixed lysates were centrifuged at 12,000×g for 15 minutes at 4℃. Thereafter,

187 the RNA-containing colorless upper aqueous phase was transferred to a new tube. The RNA was

188 precipitated by adding 250 μL of isopropyl alcohol, mixing the solution for 10 minutes at room

189 temperature, and then centrifuging it at 12,000×g for 10 minutes at 4℃ to spin down the RNA

190 pellets. After centrifugation, the supernatant was removed, and the pellets were washed twice

191 with 500 μL of 75% ethanol. Finally, the pellets were air-dried and dissolved in UltraPure

192 DNase/RNase-Free Distilled Water (10977023, ThermoFisher Scientific) by incubating them in

193 a water bath at 60℃. The RNA concentration was measured using a biophotometer.

194 **Reverse transcription and real-time PCR**

195 Total RNA was reverse transcribed to cDNA using a PrimeScripTM RT reagent Kit (RR037Q,

196 TaKaRa). First, 200-500 ng RNA was mixed with PrimeScript buffer, PrimeScript RT enzyme

197 mix I, 25 pmol oligo dT primer, and 50 pmol random 6 mers, and then it was incubated at 37℃

198 for 30 minutes followed by inactivation of reverse transcriptase at 85℃ for 10 seconds. The

199 cDNA products were diluted with DNase/RNase-free distilled water to give a final concentration

200 of 10-20 ng/μL, and then stored at -20℃.

201 We used QuantStudio 3 System (Applied Biosystems) for quantitative real-time PCR (qPCR)

202 analysis to measure the level of target gene mRNA expression. A 10-20 ng of cDNA template

203 was mixed with Fast SYBR Green Master Mix (Applied Biosystems) and 0.4 μM target gene-

204 specific primer pairs in a total volume of 10 μL. The reaction mixtures were transferred to well

205 plates and then centrifuged. The samples were denatured for 20 seconds at 95℃ followed by 40

206 cycles of the PCR stage, with the denaturing step at 95℃ for 3 seconds and the annealing and

207 extension step at 60℃ for 30 seconds. Finally, a melting curve analysis was conducted. The

208 expression levels of *Actb* were used as a loading control, and the gene-specific primer pairs are

209 listed in Table 2.

210 **Serum free fatty acid content analysis**

211 To compare serum free fatty acid levels of the CTD-fed and HFD-fed mice, we used a

212 commercial assay kit: the Free Fatty Acid Quantification Kit from BioVision (K612-100). Fifty

213 μL of serum samples were mixed with a 100 μL Reaction Mix. Then, the reactions were

214 incubated at 37℃ for 30 minutes in the dark and the OD 570 nm value was measured. The

215 sample readings were applied to the standard curve to obtain free fatty acid levels in the serum.

216 **Statistical analysis**

217 Each experiment was replicated at least three times and data were expressed as mean ± standard

218 error of the mean (SEM). Data were analyzed by Student's t-test or one-way ANOVA followed

219 by the least significant difference test (LSD) with Statistics Analysis System (Version 9.4, SAS

220 Institute Inc.); $P < 0.05$ indicated statistically significant differences.

221 # Results

222 **HFD induces autophagy impairment, insulin resistance, endoplasmic reticulum (ER)**

223 **stress, and apoptosis in adipose tissue**

224 The mice treated with 8 weeks of HFD significantly increased SQSTM1/p62 and

225 Rubicon expression, but the expression levels of LC3-II and Atg5 were unaltered (Figure 1A,B).

226 Meanwhile, the mice treated with 16 weeks of HFD had a significantly increased expression of

227 LC3-II and Atg5 (Figure 1C,D), which suggests that the late stage of autophagy might have been

228 inhibited and that the autophagosomes accumulated in a large amount to elevate the expression

229   of LC3-II on the autophagosome membrane. Further, p62 was degraded primarily by autophagy,

230   and if the lysosomal degradation of autophagosome is blocked, an accumulation of p62 is

231   expected, and so the expression of Rubicon also significantly increased.

232   There was no significant difference in serum total (Free Fatty Acids) FFAs between the

233   HFD and CTD groups at 8 and 16 weeks from the blood sample (Figure 1E). The western

234   blotting data show that insulin injection might fail to induce Akt phosphorylation (Ser473) in

235   adipose tissue from mice fed HFD for 16 weeks (Figure 1F,G). Meanwhile, we also observed the

236   marker of endoplasmic reticulum (ER) stress, CHOP, was significantly increased. One of the key

237   executioners of apoptosis, caspase-3, was activated as cleaved caspase-3 in adipose tissues from

238   mice fed with HFD (Figure 1H,I) (Kadowaki & Nishitoh, 2013; Crowley & Waterhouse, 2016).

239   We used differentiated 3T3-L1 adipocytes for FA treatment to reinforce the conclusion

240   that autophagy was inhibited in the in vivo experiment. This was done by treating 3T3-L1 cells

241   with a mixture of 0.6 mM palmitic acid (PA) and 0.6 mM oleic acid (OA) for 48 hours. We

242   observed that Bafilomycin A1 treatment given 4 hours before sampling induces less expression

243   of LC3-II protein in FA-treated cells than that in the BSA control group (Figures 2A,B).

244   **Impaired late-stage autophagy may lead to insulin resistance indirectly by ER stress or**

245   **apoptosis**

246   To investigate whether autophagy inhibition can induce insulin resistance in a cell-

247   autonomous manner, we conducted in vitro experiments using differentiated 3T3-L1 adipocytes.

248   By treating differentiated 3T3-L1 with 40 μM of CQ for 24 hours, we first addressed whether the

249   autophagy in 3T3-L1 cells was inhibited. After treatment with CQ, we observed increased LC3-

250   II and SQSTM1/p62 protein levels in 3T3-L1 cells (Figures 3A,B,C). We found that 12hosphor-

251 Akt (Ser473) in the CQ-treated group was significantly lower than that in the control (Figure

252 3A,D).

253   Interestingly, our Western blotting data showed that CQ-treated adipocytes had

254 significantly higher CHOP levels and cleaved caspase-3 than those in the control (Figure 3E,F),

255 which echoed the in vivo experiment results observed in the adipose from mice fed with HFD.

256 To further clarify whether insulin resistance was directly affected by autophagy inhibition or by

257 concomitant ER stress or apoptosis, we excluded the effects of apoptosis on cells by reducing

258 CQ concentrations. The protein levels in LC3-II in the treatment group were higher than those

259 the control group, while the levels of SQSTM1/p62 were significantly increased at

260 concentrations of 20 and 30 μM when compared to those of the control group (Figures 4A,B,C).

261   Moreover, the expression of cleaved caspase-3 did not change (Figure 4A,D). Hence, we

262 chose 20 μM dosage to determine if autophagy inhibition per se can induce insulin resistance; it

263 did not influence insulin-stimulated Akt phosphorylation in 3T3-L (Figure 4E,F).

264 **The correlation between the late-stage autophagy inhibition with insulin resistance in**

265 **adipose tissue**

266   The results indicate that 10 hours after CQ injection, the phosphorylation level induced

267 by insulin was not significantly different from that of the control group (Figure 5A,B). However,

268 the capability of insulin to generate Akt (Ser473) and GSK3β (Ser9) phosphorylation was

269 reduced 24 hours after CQ injection (Figures 5C,D,E).

270   Additionally, although the protein levels of SQSTM1/p62 and LC3-II were no difference

271 between CQ-treated and control groups (Figure 6A,B), the LC3 mRNA expression was

272 significantly decreased in adipose tissues with CQ injection (Figure 6C). These data suggested

273 that at the 24-hour post-injection of CQ, the suppression of late stage autophagy may have

274 feedback effect which resulted in reduced mRNA level of LC3.

275 **The phosphorylation of insulin signaling blocked by autophagy is not associated with the**

276 **expression of PHLPP1 and PTEN**

277   After confirming that the inhibition of late-stage autophagy is related to the occurrence of

278 insulin resistance, we further investigated the molecular mechanisms that may be involved. As it

279 was previously reported that the expression of PHLPP1 is elevated in adipose tissue of obese

280 patients and mice, which in turn leads to a decrease in phosphorylation of Akt and affected

281 insulin sensitivity (Andreozzi et al., 2011), we first checked the protein level of PHLPP1 in

282 mouse adipose treated with CQ. According to the Western blotting data, the CQ injection did not

283 increase the expression of PHLPP1 compared to that in the control group. The amount of PTEN

284 after CQ treatment was also not changed (Figure 7 A,B).

285 ## Discussion

286 Insulin resistance is considered one of the crucial factors in early-stage T2D development, which

287 can cause metabolic dysfunction in tissues. As cellular functions that may be involved in insulin

288 resistance, studies have pointed out that autophagy plays a critical role in the progression of

289 T2D, which is related to the adaptive response to intracellular stress. In particular, Cai et al.

290 (2018) observed that autophagy ablation can damage the insulin signaling transduction in

291 adipose tissues. However, the role of autophagy in adipose function and the molecular

292 mechanisms of how autophagy inhibition affects the insulin signaling pathway remain unclear.

293   HFD treatment for 8 weeks led to a blockade of late-stage autophagy in adipose, and the

294 inhibition of autophagy was observed even at the 16th week (Figures 1B,D). Rubicon's increased

295 expression was the prominent cause of suppression at the late stage, which was similar to the

296   results of Tanaka et al. (2016) and Wang et al. (2017) in hepatocytes. Fatty acid-treated cells

297   showed a significant decrease in autophagic flux (Figure 2), which doubly confirmed that

298   autophagy was inhibited and is also consistent with the clinical findings of Soussi et al. (2015)

299   Meanwhile, endoplasmic reticulum (ER) stress and apoptosis were also identified in adipose

300   tissue (Figure 1I). Studies have demonstrated that these are two effects of HFD, and Kawasaki et

301   al. (2012) further clarified that ER stress is induced by reactive oxygen species (ROS) generation

302   and inflammatory cytokines. However, Feng et al. (2011) showed that the inflammatory response

303   does not cause apoptosis. Our study brings new information that HFD might cause late-stage

304   autophagy suppression in adipose associated with Rubicon upregulation. At the same time, a

305   series of complex reactions, including insulin resistance, ER stress, and apoptosis, also occur.

306   The suppression of late-stage autophagy may damage insulin signaling transduction

307   (Figure 5D). This might be associated with the time point of sampling, or that the local injection

308   did not allow the drug to spread throughout the tissue. Interestingly, the mRNA expression of

309   LC3 in early-stage autophagy was reduced (Figure 6C), thus suggesting that the inhibition of

310   late-stage autophagy may cause feedback to decrease the mRNA level of LC3 and subsequently

311   block the early-stage autophagy. According to previous studies, if the early-stage autophagy is

312   sometimes suppressed, insulin resistance may worsen (Guo et al., 2017; Cai et al., 2018).

313   We hypothesized that some phosphatases could not be degraded because of the blocked

314   autophagic degradation, which would increase their expression and hinder the cascade of

315   phosphorylation events in the insulin signaling pathway. The protein levels of PH domain and

316   leucine-rich repeat protein phosphatase 1 (PHLPP1) and protein-tyrosine phosphatase 1B

317   (PTP1B), in adipose from obese mice or patients exhibit a significant increase compared to lean

318   animals (Andreozzi et al., 2011; Zabolotny et al., 2008). In this study, the amount of PHLPP1 did

319 not elevate as expected in the CQ-treated group but instead decreased significantly (Figure 7A).

320 It shows that autophagy suppression may not directly cause Akt phosphorylation to be restricted

321 due to increased expression of PHLPP1; conversely, it reduced the protein level of PHLPP1. In

322 this regard, we suppose that autophagy which mediated the degradation of Mir6981 was

323 inhibited, thereby leading to the abundance of Mir6981 that mitigated the protein translation of

324 PHLPP1 (Peng et al., 2019). In addition, there was no significant difference in phosphatase and

325 tensin homolog (PTEN) between the CQ-treated and control groups (Figure 7A). This indicates

326 that PTEN may also not be involved in the insulin signaling transduction blocked by autophagy

327 inhibition. In summary, autophagy inhibition at late stages blocked insulin signaling downstream

328 independent of PHLPP1 and PTEN. However, more experiments are required to establish this.

329   At a high dose (40 μM) of CQ, the insulin sensitivity in 3T3-L1 adipocytes was reduced

330 and accompanied by ER stress and apoptosis (Figure 3), which was almost identical to the

331 findings from the in vivo experiments. However, insulin signaling was still transduced normally

332 in 3T3-L1 treated with CQ, thus suggesting that autophagy suppression may not directly

333 contribute to insulin resistance. But it is also possible that the abnormality of the insulin

334 signaling pathway did not occur at the time of sampling. After CQ treatment for 24 hours, the

335 3T3-L1 adipocytes developed insulin resistance as expected, but ER stress and apoptosis were

336 also induced (Figure 3F). These results demonstrate that inhibition of late-stage autophagy per se

337 did not directly cause insulin resistance in the adipocyte. Studies have indicated that CQ blocks

338 the fusion of autophagosome and lysosome, which leads to the accumulation of a large number

339 of damaged proteins in the cytoplasm and induces ER stress.; persistent ER stress eventually

340 results in cell death (Jia et al., 2018). Moreover, van der Kallen et al. (2009) showed that the

341 relation of ER stress with insulin resistance is more evident than its relation with apoptosis. In

342 adipose, ER stress triggers activation of c-Jun N-terminal kinase (JNK) through activated inositol

343 requiring 1 alpha (IRE1α), thereby inhibiting serine phosphorylation of IRS1, and resulting in

344 insulin resistance (Zhang & Kaufman, 2008). In addition, adipocyte apoptosis contributes to

345 macrophage infiltration into adipose tissues, which increases the production of inflammatory

346 cytokines. And these cytokines can affect the insulin signaling, such as TNFα which also inhibits

347 IRS1 phosphorylation (Alkhouri et al., 2010). In summary, the suppression of late-stage

348 autophagy caused by HFD may lead to a large accumulation of impaired proteins in adipocytes,

349 which in turn leads to ER stress and apoptosis. And the latter two will eventually induce insulin

350 resistance in adipose tissue.

Conclusions

352 A long-term high-fat diet promotes insulin resistance in adipose tissue and leads to the

353 increased protein levels of Rubicon, which blocks late-stage autophagy and is accompanied by

354 endoplasmic reticulum (ER) stress and apoptosis. Among these conditions, inhibition of late-

355 stage autophagy is associated with a decrease in insulin sensitivity. However, autophagy

356 suppression may not affect the insulin signaling transduction via the pathway of PHLPP1 and

357 PTEN but instead causes insulin resistance indirectly through ER stress or the apoptosis

358 pathway.

Acknowledgements

360 We thank Nigel Daly for his diligent proofreading of this article. The authors declare no conflicts

361 of interest.

References

363

364 Alkhouri N, Gornicka A, Berk MP, Thapaliya S, Dixon LJ, Kashyap S, Schauer PR, Feldstein

365   AE. 2010. Adipocyte apoptosis, a link between obesity, insulin resistance, and hepatic

steatosis. *Journal of Biological Chemistry* 285(5): 3428-3438 DOI: 10.1074/jbc.M109.074252

Andreozzi, F, Procopio C, Greco A, Mannino GC, Miele C, Raciti GA, Iadicicco C, Beguinot F, Pontiroli AE, Hribal ML, Folli F, Sesti G. 2011. Increased levels of the Akt-specific phosphatase PH domain leucine-rich repeat protein phosphatase (PHLPP)-1 in obese participants are associated with insulin resistance. *Diabetologia* 54(7): 1879-1887 DOI: 10.1007/s00125-011-2116-6

Cai J, Pires KM, Ferhat M, Chaurasia B, Buffolo MA, Smailling R, Sargsyan A, Atkinson DL, Summers SA, Graham TE, Boudina S. 2018. Autophagy ablation in adipocytes induces insulin resistance and reveals roles for lipid peroxide and Nrf2 signaling in adipose-liver crosstalk. *Cell Reports* 25 (7): 1708-1717.e5 DOI: 10.1016/j.celrep.2018.10.040

Copps KD, White MF. 2012. Regulation of insulin sensitivity by serine/threonine phosphorylation of insulin receptor substrate proteins IRS1 and IRS2. *Diabetologia* 55(10): 2565-2582 DOI: 10.1007/s00125-012-2644-8

Crowley LC, Waterhouse NJ. 2016. Detecting cleaved caspase-3 in apoptotic cells by flow cytometry. *Cold Spring Harbor Protocols* 11 DOI: 10.1101/pdb.prot087312.

Fazakerley DJ, Krycer JR, Kearney AL, Hocking SL, James DE. 2019. Muscle and adipose tissue insulin resistance: malady without mechanism? *Journal of Lipid Research* 60(10): 1720-1732 DOI: 10.1194/jlr.R087510

Feng D, Tang Y, Kwon H, Zong H, Hawkins M, Kitsis RN, Pessin JE. 2011. High-fat diet-induced adipocyte cell death occurs through a Cyclophilin D intrinsic signaling pathway independent of adipose tissue inflammation. *Diabetes* 60(8): 2134-2143 DOI: 10.2337/db10-1411

389 Glick D, Barth S, Macleod KF. 2010. Autophagy: cellular and molecular mechanisms. *The*

390   *Journal of Pathology* 221(1): 3-12 DOI: 10.1002/path.2697.

391 Guo Q, Xu L, Li H, Sun H, Wu S, Zhou B. 2017. 4-PBA reverses autophagic dysfunction and

392   improves insulin sensitivity in adipose tissue of obese mice via Akt/mTOR signaling.

393   *Biochemical and Biophysical Research Communication* 484(3): 529-535 DOI:

394   10.1016/j.bbrc.2017.01.10616.

395 Hanada T, Noda NN, Satomi Y, Ichimura Y, Fujioka Y, Takao T, Inagaki F, Ohsumi Y. 2007.

396   The Atg12-Atg5 conjugate has a novel E3-like activity for protein lipidation in

397   autophagy. *Journal of Biological Chemistry* 282(52): 37298-302 DOI:

398   10.1074/jbc.C700195200

399 Jia B, Xue Y, Yan X, Li J, Wu Y, Guo R, Zhang J, Zhang L, Li Y, Liu Y, Sun L. 2018.

400   Autophagy inhibitor chloroquine induces apoptosis of cholangiocarcinoma cells via

401   endoplasmic reticulum stress. *Oncology Letters* 16(3): 3509–3516 DOI:

402   10.3892/ol.2018.9131

403 Kabeya Y, Mizushima N, Yamamoto A, Oshitani-Okamoto S, Ohsumi Y, Yoshimori T. 2004.

404   LC3, GABARAP and GATE16 localize to autophagosomal membrane depending on

405   form-II formation. *Journal of Cell Science* 117: 2805-2812.

406 Kadowaki H, Nishitoh H. 2013. Signaling pathways from the endoplasmic reticulum and their

407   roles in disease. *Genes (Basel)* 4(3): 306-333 DOI: 10.3390/genes4030306.

408 Kawasaki N, Asada R, Saito A, Kanemoto S, Imaizumi K. 2012. Obesity induced endoplasmic

409   reticulum stress causes chronic inflammation in adipose tissue. *Scientific Reports* 2: 799

410   DOI: 10.1038/srep00799

411 Kosacka J, Kern M, Klöting N, Paeschke S, Rudich A, Haim Y, Gericke M, Serke H, Stumvoll

412   M, Bechmann I, Nowicki M, Blüher M. 2015. Autophagy in adipose tissue of patients

413   with obesity and type 2 diabetes. *Molecular and Cellular Endocrinology* 409: 21-32 DOI:

414   10.1016/j.mce.2015.03.015

415 Loos, B., du Toit, A., & Hofmeyr, J. H. (2014). Defining and measuring autophagosome flux—

416   concept and reality. Autophagy,10(11),2087–2096. DOI:10.4161/15548627.2014.973338

417 Mizushima N. 2007. Autophagy: process and function. *Genes and Development* 21(22): 2861-73

418 Molina JR, Agarwal NK, Morales FC, Hayashi Y. Aldape KD, Cote G, Georgescu MM. 2012.

419   PTEN, NHERF1 and PHLPP form a tumor suppressor network that is disabled in

420   glioblastoma. *Oncogene* 31(10): 1264-1274 DOI:10.1038/onc.2011.324

421 Moulis M, Vindis C. 2017. Methods for Measuring Autophagy in Mice. Cells, 6(2), 14.

422   DOI:10.3390/cells6020014

423 Ozcan U, Cao Q, Yilmaz E, Lee AH, Iwakoshi NN, Ozdelen E, Tuncman G, Görgün C,

424   Glimcher LH, Hotamisligil GS. Endoplasmic reticulum stress links obesity, insulin

425   action, and type 2 diabetes. Science. 2004 Oct 15;306(5695):457-61. DOI:

426   10.1126/science.1103160.

427 Pal A, Barber TM, Van de Bunt M, Rudge SA, Zhang Q, Lanchlan, KL, Cooper NS, Linden H,

428   Levy JC, Wakelam MJO, Walker L, Karpe F, Gloyn AL. 2012. PTEN mutations as a

429   cause of constitutive insulin sensitivity and obesity. *The New England Journal of*

430   *Medicine* 367(11): 1002-1011 DOI: 10.1056/NEJMoa1113966

431 Peng M, Wang J, Tian Z, Zhang D, Jin H, Liu C, Xu J, Li J, Hua X, Xu J, Huang C, Huang C.

432   2019. Autophagy-mediated Mir6981 degradation exhibits CDKN1B promotion of

433   PHLPP1   protein   translation.   *Autophagy*   15(9):   1523-1538   DOI:
434   10.1080/15548627.2019.1586254

435   Rodríguez A , Gómez-Ambrosi J, Catalán V, Rotellar F, Valentí V, Silva C, Mugueta C, Pulido
436   M R, Vázquez R, Salvador J, Malagón MM, Colina I, Frühbeck G. 2012. The ghrelin O-
437   acyltransferase-ghrelin system reduces TNF-α-induced apoptosis and autophagy in
438   human visceral adipocytes. *Diabetologia* 55(11): 3038-50 DOI: 10.1007/s00125-012-
439   2671-5

440   Romanov J, Walczak M, Ibiricu I, Schüchner S, Ogris E, Kraft C, Martens S. 2012. Mechanism
441   and functions of membrane binding by the Atg5-Atg12/Atg16 complex during
442   autophagosome formation. *EMBO Journal* 31(22): 4304-4317 DOI:
443   10.1038/emboj.2012.278

444   Soussi H, Reggio S, Alili R, Prado C, Mutel S, Pini M, Rouault C, Clément K, Dugail I. 2015.
445   DAPK2 downregulation associates with attenuated adipocyte autophagic clearance in
446   human obesity. *Diabetes* 64(10): 3452-3463 DOI: 10.2337/db14-1933

447   Tanaka S, Hikita H, Tatsumi T, Sakamori R, Nozaki Y, Sakane S, Shiode Y, Nakabori T, Saito
448   Y, Hiramatsu N, Tabata K, Kawabata T, Hamasaki M, Eguchi H, Nagano H, Yoshimori
449   T, Takehara T. 2016. Rubicon inhibits autophagy and accelerates hepatocyte apoptosis
450   and lipid accumulation in nonalcoholic fatty liver disease in mice. *Hepatology* 64(6):
451   1994-2014 DOI: 10.1002/hep.28820

452   van der Kallen, CJH, van Greevenbroek MMJ, Stehouwer CDA Schalkwijk CG. 2009.
453   Endoplasmic reticulum stress-induced apoptosis in the development of diabetes: Is there a
454   role for adipose tissue and liver? *Apoptosis* 14(2): 1424-1434 DOI: 10.1007/s10495-009-
455   0400-4

456 Wang ME, Singh BK, Hsu MC, Huang C, Yen P, Wu LS, Jong D, Chiu C. 2017, Increasing

457   dietary medium-chain fatty acid ratio mitigates high-fat diet induced non-alcoholic

458   steatohepatitis by regulating autophagy. *Scientific Reports* 7: 13999

459   DOI:10.1038/s41598-017-14376-y

460 Yang Z, Klionsky DJ. 2009. Mammalian autophagy: Core molecular machinery and signaling

461   regulation. *Current Opinion in Cell Biology* 22(2): 124-131 DOI:

462   10.1016/j.ceb.2009.11.014

463 Yin J, Wang Y, Gu L, Fan N, Ma Y, Peng Y. 2015. Palmitate induces endoplasmic reticulum

464   stress and autophagy in mature adipocytes: Implications for apoptosis and inflammation.

465   *International Journal of Molecular Medicine* 35(4): 932-940 DOI:

466   10.3892/ijmm.2015.2085

467 Zabolotny JM, Kim YB, Welsh LA, Kershaw EE, Neel BG, Kahn BB. 2008. Protein-tyrosine

468   phosphatase 1B expression is induced by inflammation in vivo. *Journal of Biological*

469   *Chemistry* 283(21): 14230-14241 DOI: 10.1074/jbc.M800061200

470 Zhang K, Kaufman RJ. 2008. From endoplasmic-reticulum stress to the inflammatory response.

471   *Nature* 454(7203): 455-462 DOI: 10.1038/nature07203

472 Zhou L, Zhang J, Fang Q, Liu M, Liu X, Jia W, Dong LQ, Liu F. 2009. Autophagy-mediated

473   insulin receptor down-regulation contributes to endoplasmic reticulum stress-induced

474   insulin resistance. *Molecular Pharmacology* 76(3): 596-603 DOI:

475   10.1124/mol.109.057067

476

Figure 1

Altered autophagy, insulin resistance, and ER stress in adipose tissues from mice fed with 8- and 16-week HFD

Figure 1. Altered autophagy, insulin resistance, and ER stress in adipose tissues from mice fed with 8- and 16-week HFD. The 12-week-old male B6 mice were fed with either the control diet or HFD for 8 weeks (A,B) and 16 weeks (C,D). T t he figure shows the immunoblots and the densitometric qua n tifications of SQSTM1/p62, LC3, Rubicon, and Atg5 expression by Western blotting. Values are mean ± SEM (n=4). The serum-free fatty acid levels between CTD-fed and HFD-fed mice were analyzed using a commercial assay kit (E). Values are mean ± SEM (8 weeks: n=4 and 16 weeks: n=6). n.s.: no significant difference. The phospho-Akt (Ser473) levels of adipose tissues from mice injected with or without insulin (0.5 IU/kg body weight I.P., 30 minutes) were analyzed at the 16th week using Western blotting (F,G). Values are mean ± SEM (n=6). Different letters are considered statistically significant difference by one-way ANOVA and least significant difference (LSD) test, P < 0.05. Male B6 mice were fed with either the control diet or HFD for 16 weeks (H,I). The figure shows the immunoblots and the densitometric quantifications of CHOP and cleaved caspase-3 expression by Western blotting. Values are mean ± SEM (n=6). * indicates statistical significance, P < 0.05.
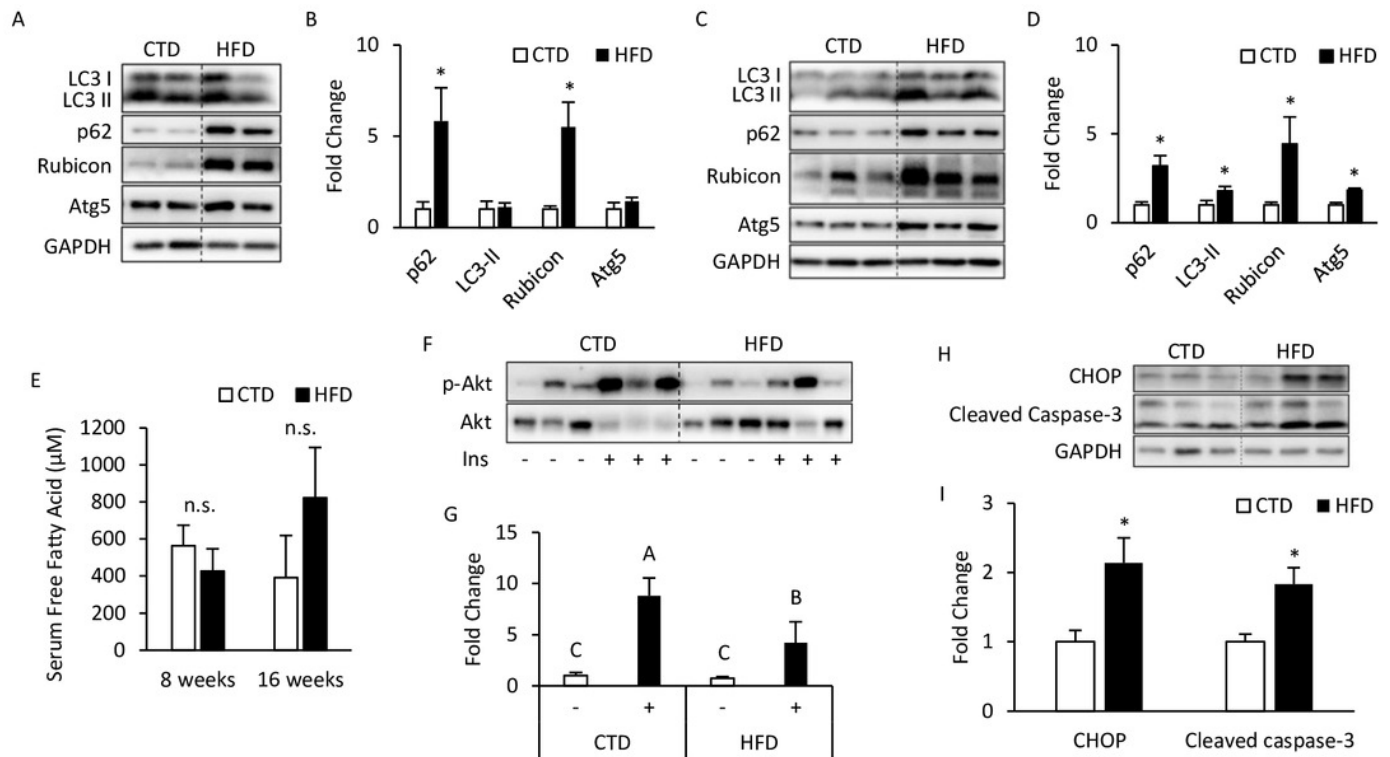
Figure 2

Free fatty acids (FFAs) impaired the autophagic flux in differentiated 3T3-L1 adipocytes

Figure 2. Free fatty acids (FFAs) impaired the autophagic flux in differentiated 3T3-L1 adipocytes. The Bafilomycin A1-induced LC3 II protein accumulation in 48-hour BSA- and FFA-(0.6 mM PA + 0.6 mM OA) loaded 3T3-L1 adipocytes were analyzed using Western blotting. The immunoblots (A), and calculated fold change of LC3 II protein levels were presented (B). For densitometric analyses, GAPDH was used as the loading control. Values are mean ± SEM (n=3). * indicates statistical significance, P < 0.05.
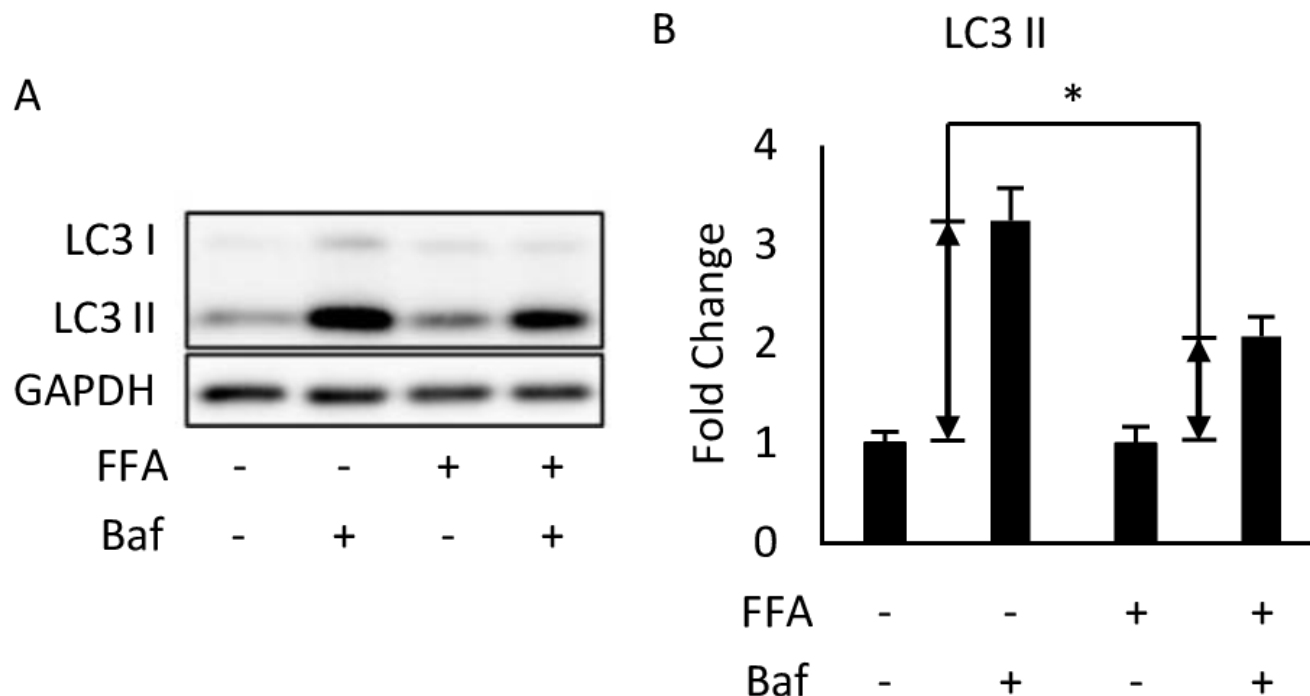
Figure 3

Autophagy inhibition, insulin resistance, ER stress and apoptosis were found in 3T3-L1 after CQ treatment for 24 hours.

Figure 3. Autophagy inhibition, insulin resistance, ER stress and apoptosis were found in 3T3-L1 after CQ treatment for 24 hours. The differentiated 3T3-L1 adipocyte was treated with 40 µM CQ for 24 hours, and with 40 nM insulin for 15 minutes before sampling. SQSTM1/p62, LC3 and p-Akt/Akt immunoblots (A) and densitometric quantifications (B,C,D). The differentiated 3T3-L1 adipocyte was treated with 40 µM CQ for 24 hours. CHOP and cleaved caspase-3 immunoblot (E) and densitometric quantifications (F). For densitometric analyses of Western blotting data, GAPDH was used as the loading control. Values are mean ± SEM (n=3). Different letters are considered statistically significant difference by one-way ANOVA and least significant difference (LSD) test, $P < 0.05$.

A

B

LC3-II

C

p62

D

p-Akt

E

F
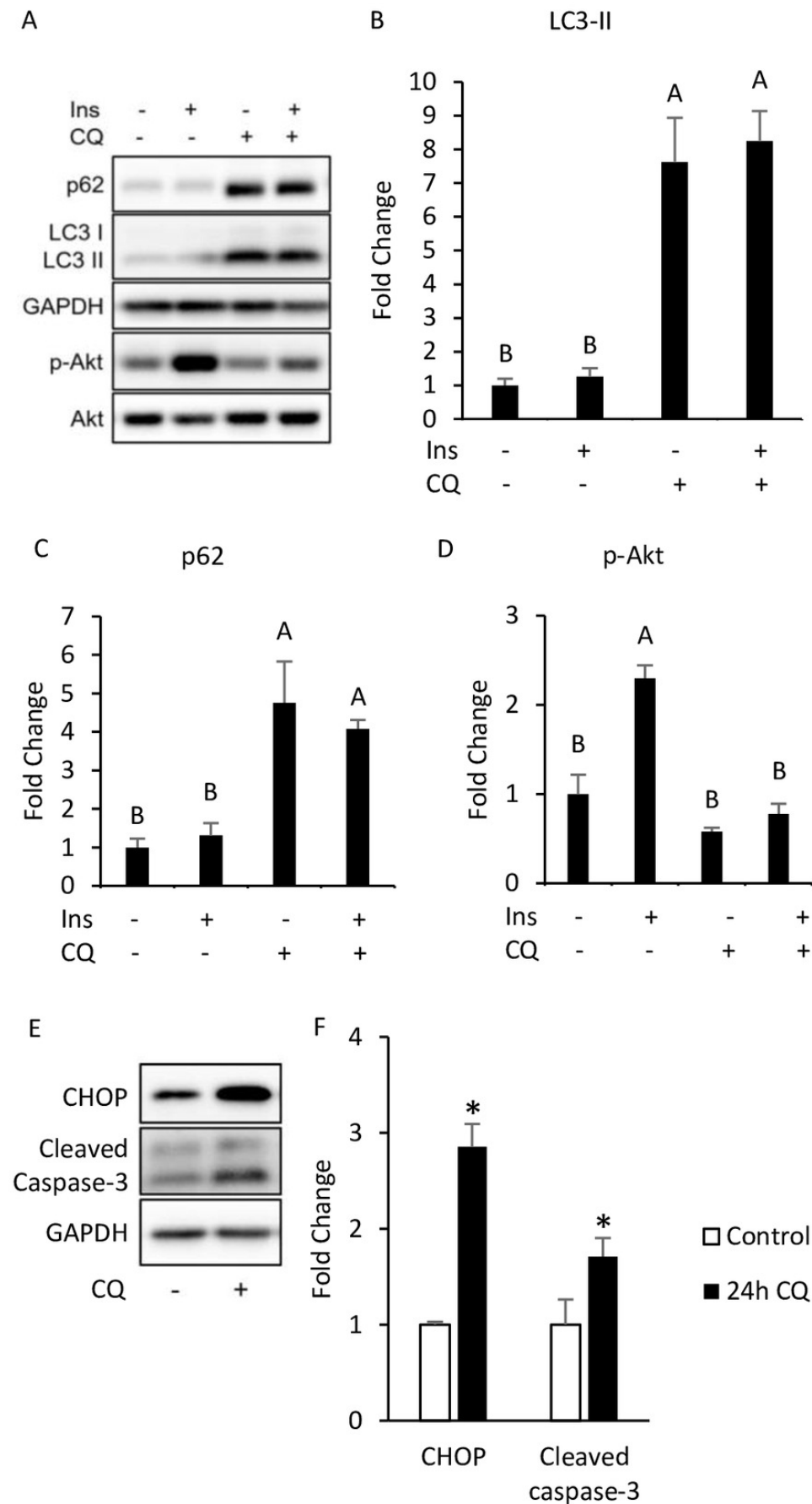
Figure 4

Dose-response experiment of CQ treatment in 3T3-L1 cells and insulin resistance, ER stress, and apoptosis were observed in 3T3-L1 after 20 µM CQ treatment for 48 hours.

Figure 4. Dose-response experiment of CQ treatment in 3T3-L1 cells and insulin resistance, ER stress, and apoptosis were observed in 3T3-L1 after 20 µM CQ treatment for 48 hours. The differentiated 3T3-L1 adipocyte was treated with 10, 20, and 30 µM CQ, for 24 hours (A). The figure shows SQSTM1/p62 (B), LC3 (C), and cleaved caspase-3 (D) immunoblots and densitometric quantifications. The differentiated 3T3-L1 adipocyte was treated with 20 µM CQ for 24 hours and with 40 nM insulin for 15 minutes before sampling. The phospho-Akt (Ser473) and total Akt levels of 3T3-L1 adipocyte were analyzed using Western blotting (E,F). GAPDH was used as the loading control. Values are mean ± SEM (n=3). Different letters are considered statistically significant difference by one-way ANOVA and least significant difference (LSD) test, $P < 0.05$. n.s.: no significant difference.
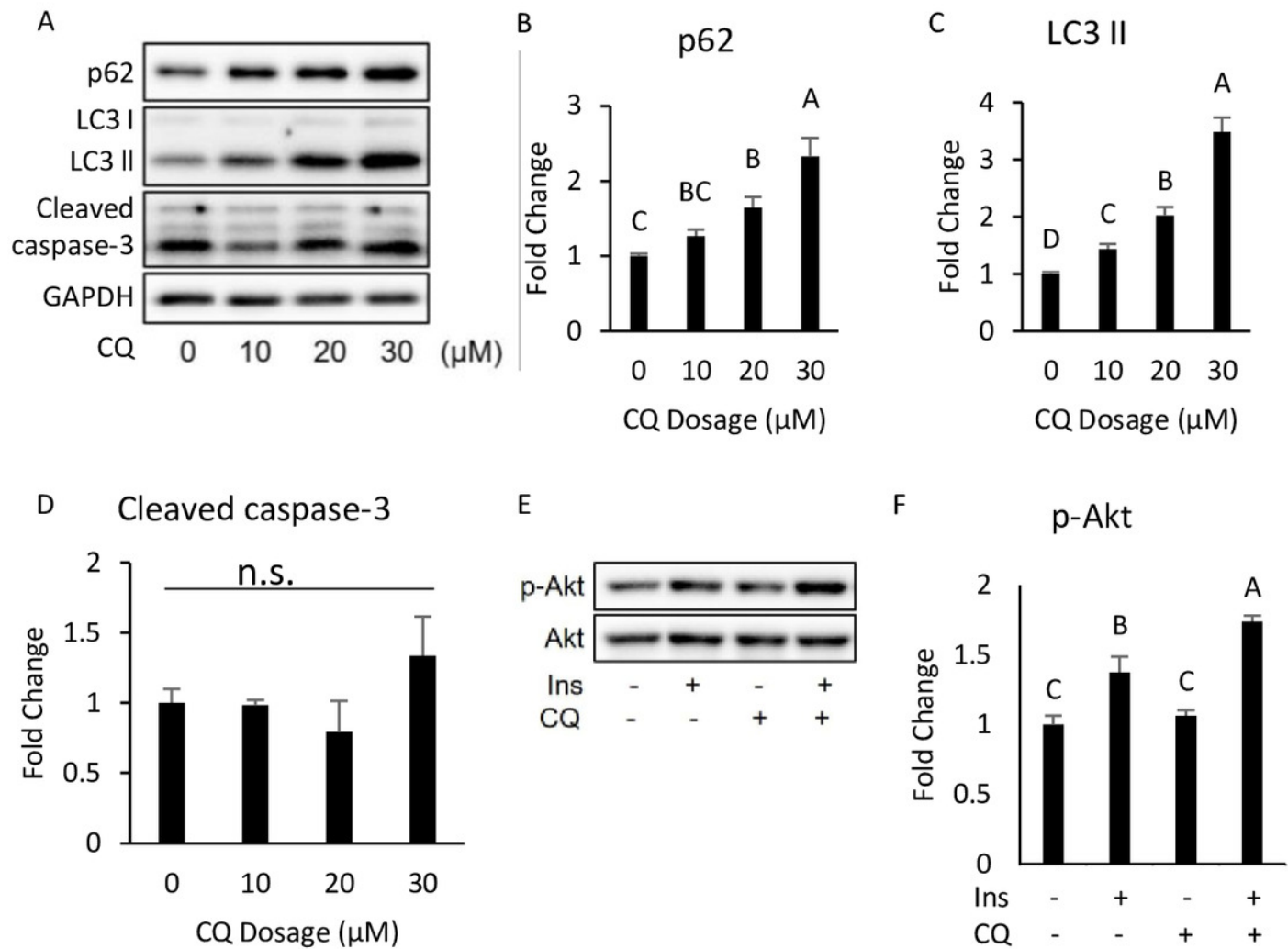
Figure 5

The insulin signaling pathway after chloroquine (CQ) treatment for 10 hours and 24 hours.

Figure 5. The insulin signaling pathway after chloroquine (CQ) treatment for 10 hours and 24 hours. B6 mice were injected with PBS or CQ into epididymal adipose tissue for 10 hours (A,B) and 24 hours (C,D,E) mice injected with or without I.P. insulin (0.5 IU/kg body weight, 30 minutes) before sacrifice. The phospho-Akt (Ser473) and total Akt levels of adipose tissues were analyzed with Western blotting. Blotting and quantitative data of p-Akt/Akt and p-GSK3β/ GSK3β were presented. Values are mean ± SEM (n=4) (A) (n=6) (C). Different letters are considered statistically significant difference by one-way ANOVA and least significant difference (LSD) test, P < 0.05. GAPDH was used as the loading control. The LC3B mRNA level in 24-hour PBS- and CQ-treated adipose was measured using qPCR analysis. For data quantification, the housekeeping gene ACTB was used as the internal control. Values are mean ± SEM (n=6). * indicates statistical significance, P < 0.05. n.s.: no significant difference.
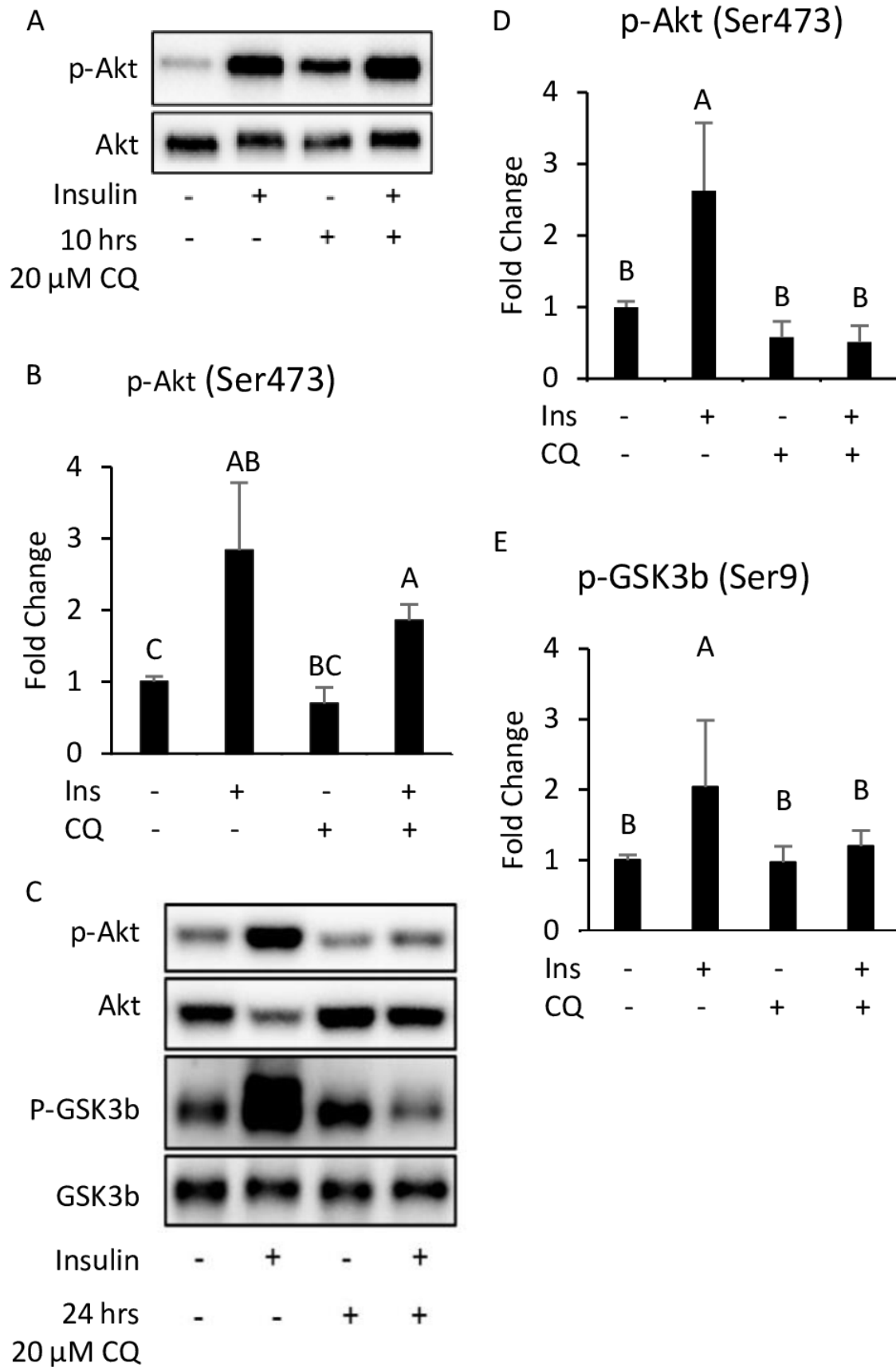
Figure 6

The suppression of late-stage autophagy may have feedback effect which resulted in reduced mRNA level of LC3B.

Figure 6. The suppression of late-stage autophagy may have feedback effect which resulted in reduced mRNA level of LC3B. B6 mice were injected with PBS or CQ into epididymal adipose tissue for 24 hours. Representative SQSTM1/p62 and LC3 immunoblots and densitometric quantifications (A,B). For densitometric analyses of Western blotting data, GAPDH was used as loading control. The LC3B mRNA level in 24-hour PBS- and CQ-treated adipose was measured using qPCR analysis (C). For data quantification, the housekeeping gene ACTB was used as the internal control. Values are mean ± SEM (n=6). * indicates statistical significance, P < 0.05. n.s.: no significant difference.
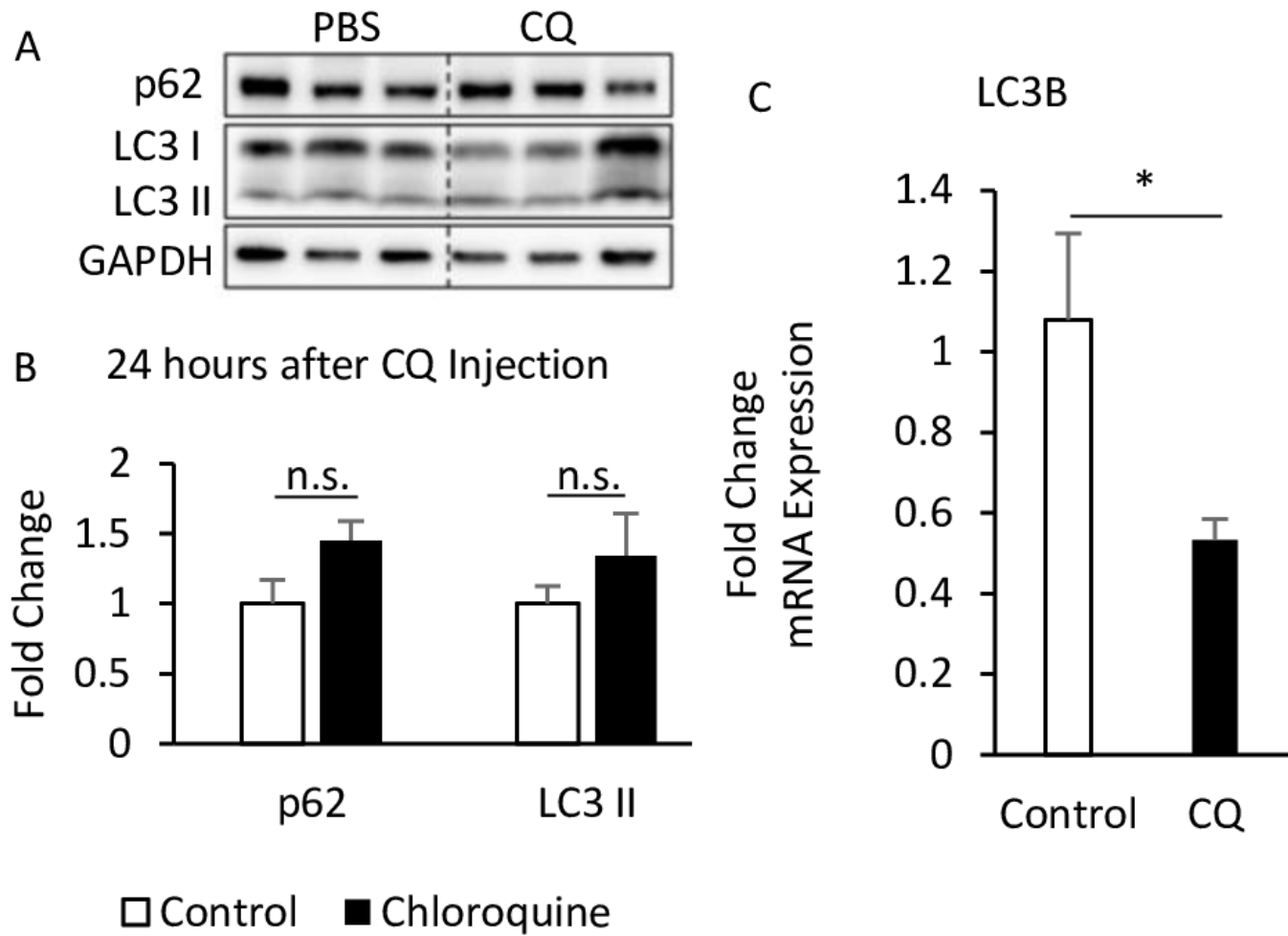
Figure 7

Autophagy may regulate insulin-stimulated signal transduction without associated with PHLPP1 and PTEN

Figure 7. Autophagy may regulate insulin-stimulated signal transduction without associated with PHLPP1 and PTEN. The PHLPP1 and PTEN level of PBS- and CQ-injected mouse adipose via Western blotting. * indicates statistical significance, P <0.05. Quantitative data (A) and western blotting (B) of PTEN were presented. For densitometric analyses of Western blotting data, GAPDH was used as the loading control. Values are mean ± SEM (n=3). n.s.: no significant difference.
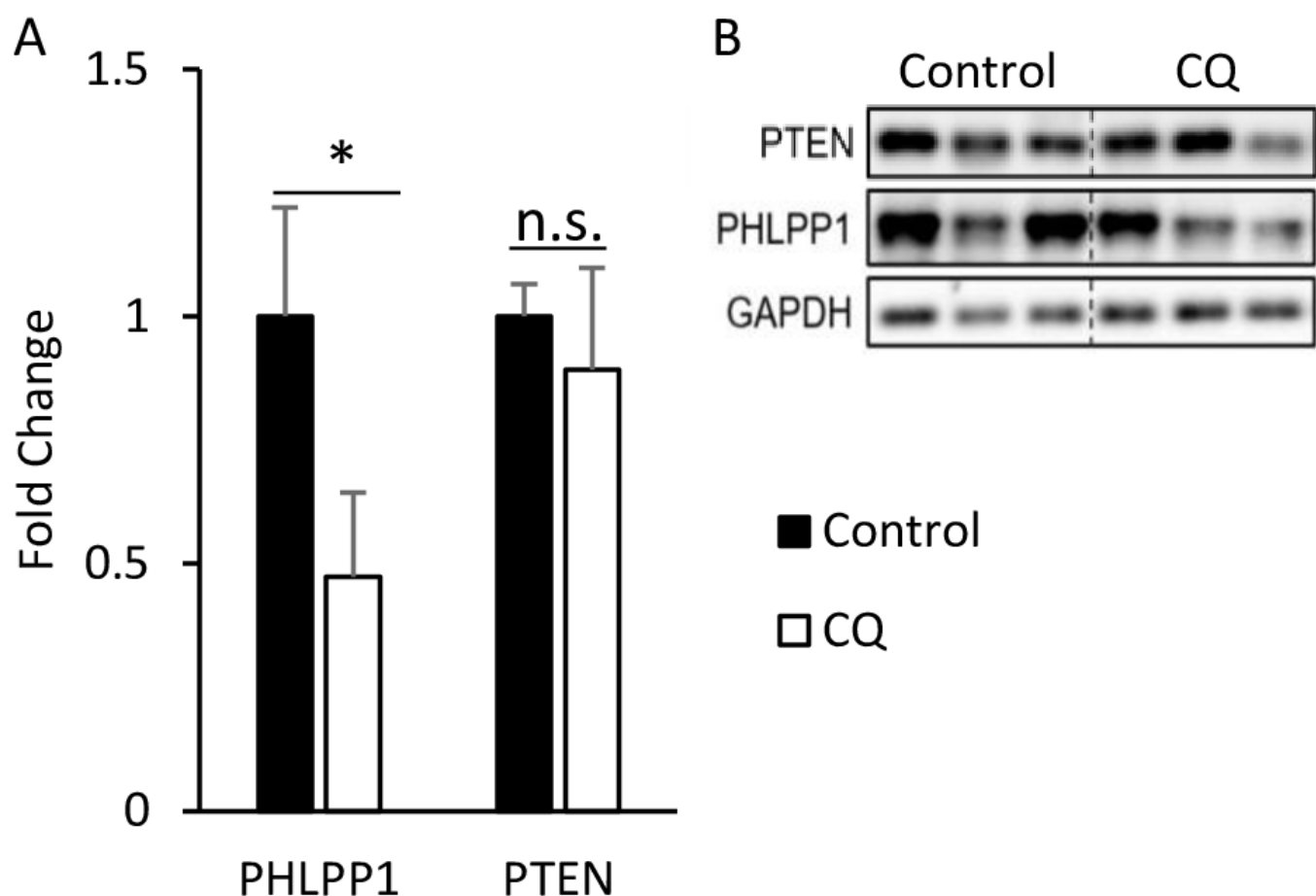
The antibodies used in the study

1 Table 1. The antibodies used in the study

Antibody Name	Company Product	Number
Anti-Akt	Cell Signaling Technology	4691S
Anti-phospho-Akt Ser 473	Cell Signaling Technology	4060S
Anti-ATG5	Cell Signaling Technology	12994S
Anti-CHOP	Cell Signaling Technology	2895S
Anti-cleaved caspase 3	Cell Signaling Technology	9664S
Anti-GAPDH	Cell Signaling Technology	2118S
Anti-GSK-3β	Cell Signaling Technology	3915S
Anti-phospho-GSK-3β S9	Cell Signaling Technology	5558S
Anti-LC3	Cell Signaling Technology	2775S
Anti-PHLPP1	Merck Millipore	07-1341
Anti-PTEN	Cell Signaling Technology	9559S
Anti-Rubicon	Cell Signaling Technology	8465S
Anti-SQSTM1/p62	Abcam	ab109012
Goat anti-rabbit IgG-HRP	Santa Cruz Biotechnology	sc-2004

The primer pairs used in qPCR analysis

1   Table 2. The primer pairs used in qPCR analysis

Gene Name	Forward (5' to 3')	Reverse (5' to 3')
Map1lc3b	GGAGCTTTGAACAAAGAGTGGAA	GGTCAGGCACCAGGAACTTG
Actb	GTGCGTGACATCAAAGAG	CAAGAAGGAAGGCTGGAA